

ORIGINAL ARTICLE

Erasure of methylation imprint at the promoter and CTCF-binding site upstream of *H19* in human testicular germ cell tumors of adolescents indicate their fetal germ cell origin

T Kawakami¹, C Zhang¹, Y Okada and K Okamoto

Department of Urology, Shiga University of Medical Science, Otsu, Shiga, Japan

Genome-wide epigenetic modification plays a crucial role in regulating genome functions at critical stages of development. In particular, DNA methylation is known to be reprogrammed on a genome-wide level in germ cells and in preimplantation embryos, although it is relatively stable in somatic cells. In this reprogramming process, the genome becomes demethylated, and methylated *de novo* during later stages of development. Reprogramming of DNA methylation in male germ cells has not been fully investigated. Testicular germ cell tumors (TGCTs) possess a pluripotential nature and display protean histology from germ cells to embryonal and somatic cell differentiation. These properties make TGCT a unique model for studying germ cell development and gametogenesis in respect of DNA reprogramming. In order to obtain an insight into the epigenetic dynamics of TGCTs, we conducted a comprehensive analysis of differential methylated regions (DMRs) on *H19* and *IGF2* in TGCTs compared with testicular malignant lymphomas. In the present study, we show that methylation imprint at the promoter and CTCF-binding site upstream of *H19* was completely erased in both seminomatous and non-seminomatous TGCTs, whereas differential methylation was observed in testicular lymphomas. The erasure of methylation imprint was also observed in TGCTs with malignant transformation. We found biallelic unmethylation at the promoter and the CTCF-binding site upstream of *H19* is required, but not sufficient for the biallelic expression of *H19* in TGCTs. These data suggest that factors other than methylation contribute to transcriptional regulation of imprinted genes in TGCTs. The present data have shown that TGCTs carry distinctive epigenetic profiles at the core-imprinting domain of *H19/IGF2* from other neoplasms of somatic cell origin. The data also suggest that both seminomatous and non-seminomatous TGCTs carry methylation profiles similar to fetal germ cells, but not adult germ cells, indicating the origin of TGCTs as fetal germ cells.

Oncogene (2006) 25, 3225–3236. doi:10.1038/sj.onc.1209362; published online 23 January 2006

Keywords: testicular cancer; methylation; imprinting; DNA reprogramming; *H19*

Introduction

Testicular germ cell tumors (TGCTs) are the most common cancer in males aged 20–35 years. TGCTs are classified into two major histological subgroups, seminoma and non-seminoma: both are suggested to arise from a precursor, known as carcinoma *in situ* (Skakkebaek, 1972). Non-seminomatous TGCTs demonstrate embryonal and extraembryonal differentiation patterns, which include primitive zygotic (embryonal carcinoma), embryonal-like somatic differentiated (teratoma) and extraembryonally differentiated (choriocarcinoma, yolk sac tumor) phenotypes (Ulbright, 1993).

Epidemiological (Moller, 1989), morphological (Skakkebaek *et al.*, 1987; Holstein, 1993) and immunohistochemical data (Jorgensen *et al.*, 1995) suggest that TGCTs arise from fetal germ cells, probably primordial germ cells (PGCs). In particular, seminoma cells mimic early germ cells, probably PGCs or gonocytes (Skakkebaek *et al.*, 1987). Recent immunohistochemical data demonstrated that seminoma and embryonal carcinoma cells are positive for *OCT3/4*, suggesting TGCTs derive from PGCs (Looijenga *et al.*, 2003; Rajpert-De Meyts *et al.*, 2004; Oosterhuis and Looijenga, 2005).

The formation of DNA methylation patterns is one of the epigenetic events underlying the development of various tissues in mammals (Shiota and Yanagimachi, 2002). DNA methylation is involved in gene silencing, switching and stabilizing, and chromatin remodeling (Okano *et al.*, 1999; Li, 2002). In mammals, DNA methylation is known to be reprogrammed on a genome-wide level in germ cells and in preimplantation embryos, although it is relatively stable in somatic cells (Reik *et al.*, 2001). In this reprogramming process, the genome becomes demethylated, and methylated *de novo* during later stages of development. It has been shown that complete epigenetic reprogramming (genome-wide demethylation) occurs within 1 day of the developmental period of mouse PGCs after reaching the genital ridge (Hajkova *et al.*, 2002; Lee *et al.*, 2002).

Correspondence: Dr K Okamoto, Department of Urology, Shiga University of Medical Science, Otsu, Shiga 520-2192, Japan.
E-mail: keisei@belle.shiga-med.ac.jp

¹These authors have equally contributed to this work.

Received 5 August 2005; revised 17 November 2005; accepted 30 November 2005; published online 23 January 2006

A genome-wide methylation study using restriction landmark genome scanning demonstrates that seminomatous TGCTs show significantly low levels of methylation (Smiraglia *et al.*, 2002). We have already shown that TGCTs carry unique methylation profiles on the X-chromosome (Kawakami *et al.*, 2003, 2004a). We demonstrated that three X-linked genes (*AR*, *FMRI* and *GPC3*) on supernumerical X-chromosomes in both seminomatous and non-seminomatous TGCTs are predominantly unmethylated, regardless of whether *XIST* is expressed (Kawakami *et al.*, 2003). The data indicate that the roles of *XIST* expression in TGCTs are distinct from those in female-inactive X-chromosomes where the X-linked genes (*AR*, *FMRI* and *GPC3*) are silenced via methylation of the promoter (Allen *et al.*, 1992; Kirchgessner *et al.*, 1995; Huber *et al.*, 1999; Kawakami *et al.*, 2004b). We have also shown that the unmethylated profile is present at the 5' end of the *XIST* gene in both seminomatous and non-seminomatous TGCTs, regardless of *XIST* expression (Kawakami *et al.*, 2004a). A similar consistent unmethylated profile is observed at *SYCP1*, a cancer testis antigen gene on chromosome 1, in both seminomatous and non-seminomatous TGCTs (Zhang *et al.*, 2005). On the contrary, 5' ends of *MAGEA1* and *MAGEA3*, cancer testis antigen genes on the X-chromosome, are unmethylated in seminomatous TGCTs, regardless of whether *MAGEA1* and *MAGEA3* are expressed, but methylated in non-seminomatous TGCTs in accordance with an absence of expression (Zhang *et al.*, 2005).

Consistent unmethylated DNA profiles in seminomatous TGCTs imply that methylation may not be the primary control mechanism for gene transcription in seminomatous TGCTs.

The data mentioned above suggests that reprogramming of DNA methylation observed in fetal germ cells or PGCs might occur in TGCTs, particularly in seminomatous TGCTs. However, there is no direct evidence that TGCTs possess DNA methylation profile same as that in fetal germ cells.

Genomic imprinting is an epigenetic mechanism causing functional differences between paternal and maternal genomes, and plays an essential role in mammalian development. Differential methylation of cytosine residues in CpG dinucleotides in critical regions of imprinted genes is part of the imprinting process differentiating paternal and maternal alleles (Barlow, 1993). Imprinted genes have been well analysed in terms of genome reprogramming, and it is widely accepted that imprinting memories are erased in PGCs and that DNA methylation is an important factor in this process (Grant *et al.*, 1992; Kafri *et al.*, 1992; Brandeis *et al.*, 1993; Szabo and Mann, 1995b; Kato *et al.*, 1999). Maternally expressed *H19* is one of the best-characterized imprinted genes. The 5' region of *H19* is methylated only on the paternal allele in both mouse (Bartolomei *et al.*, 1993; Ferguson-Smith *et al.*, 1993) and human (Jinno *et al.*, 1996). This region is regarded as a key domain in the control of imprinting at this locus (Thorvaldsen *et al.*, 1998). The DMR of *H19* contains seven potential CTCF-binding sites. This area is

differentially methylated in most normal tissues, with the paternal allele being methylated and the maternal allele being unmethylated (Zhang *et al.*, 1993; Jinno *et al.*, 1996; Vu *et al.*, 2000). Takai *et al.* (2001) have shown that only the sixth of the seven CTCF-binding sites demonstrates allele-specific methylation. Expression of imprinted genes, such as *H19*, in the germ line become biallelic at day 11.5 of mouse embryonic development (Szabo and Mann, 1995b; Villar *et al.*, 1995). Loss of allele-specific methylation imprints has also been observed in both male and female PGCs of the mouse (Tada *et al.*, 1998). These lines of data support the hypothesis that pre-existing imprints are erased in the germ line by this stage. By analysing individual micro-dissected human male germ cells at different stages of development, Kerjean *et al.*, have shown that fetal spermatogonia are predominantly unmethylated at the differential methylated regions (DMRs) of *H19*, although adult germ cells of testis (spermatogonia on ward) demonstrate significant methylation at this region.

In order to obtain an insight into the epigenetic dynamics in TGCTs, we conducted a comprehensive analysis of DMRs on *H19* and *IGF2* in a series of TGCTs compared with testicular malignant lymphomas.

Results

Methylation imprint at the promoter and the CTCF-binding site upstream of H19 is completely erased in both seminomatous and non-seminomatous TGCTs, but not in testicular lymphomas

First, we studied the methylation profile of the promoter and the sixth CTCF-binding site upstream of *H19* in TGCT tissues in comparison with testicular lymphoma tissues. To enable us to determine the methylation status of individual CpG sites, we cloned and sequenced bisulfite-treated DNA. We incorporated two TGCT tissues with malignant transformation to see whether the malignant transformation in TGCTs causes methylation imprint alterations. Figures 1a and 2a demonstrate analysed CpG sites at the promoter and the sixth CTCF-binding site upstream of *H19* in different samples, respectively. The promoter region includes two polymorphic sites (Figure 1a). Eight out of the 19 samples were informative for differentiating the two alleles of this region. The region encompassing the sixth CTCF-binding site includes three polymorphic sites (Figure 2a). Eleven of the 19 samples were informative for differentiating the two alleles of this region. In peripheral blood leukocytes (PBLs), differential methylation was observed both at the promoter and the CTCF-binding site upstream of *H19* (Figures 1b and 2b). In normal testicular tissues, the promoter and the CTCF-binding site were differentially methylated (Figure 1b), although one clone of the unmethylated allele of NT1 and NT2 showed methylation at the CTCF-binding site (Figure 2b). Testicular lymphoma tissues also

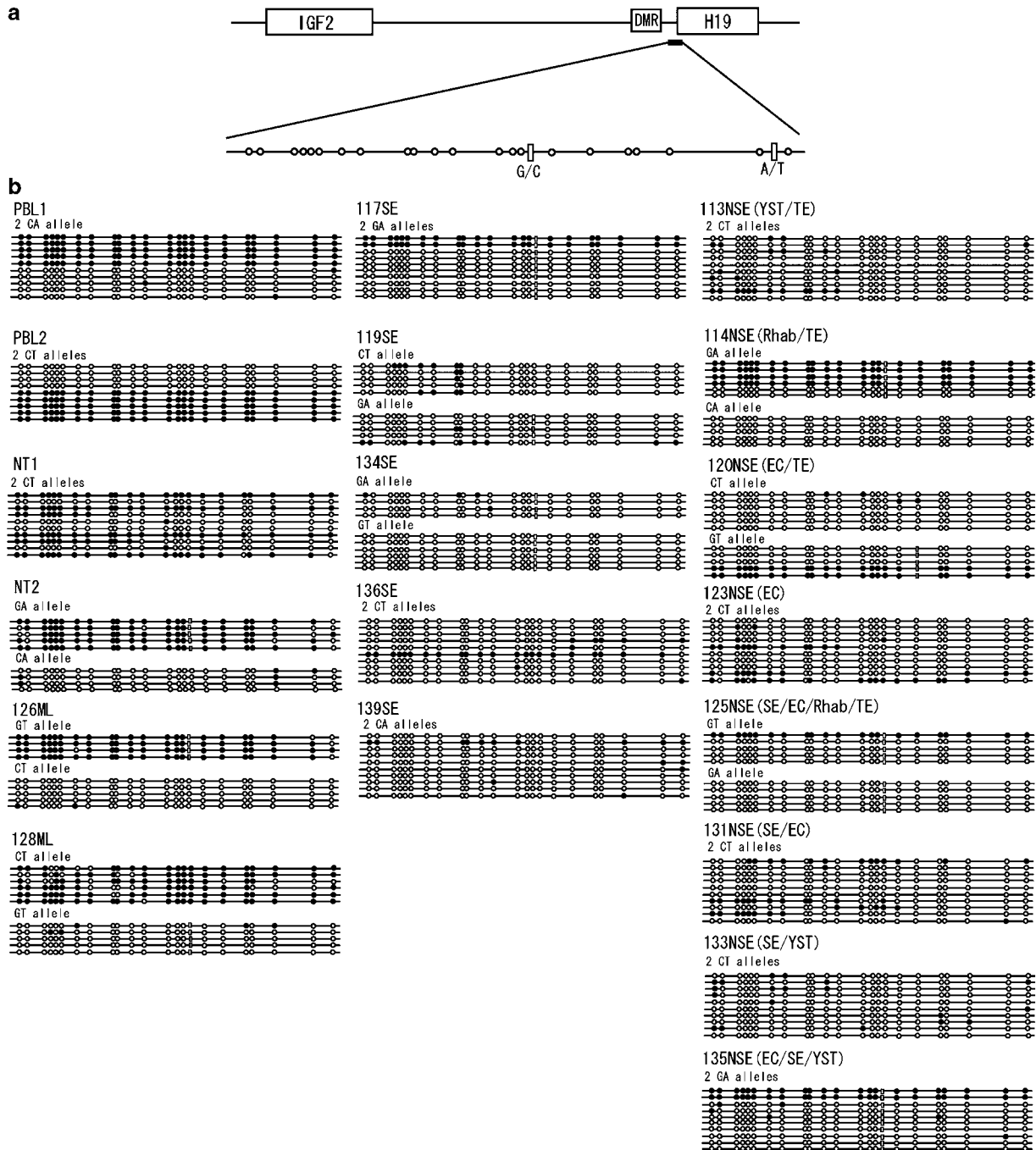


Figure 1 Methylation status of individual CpG sites at the promoter region of *H19*. Distribution of CpG dinucleotides at the promoter region of *H19*. The 22 CpG sites analysed by bisulfite sequencing are magnified and represented by open circles. (a) The locations of polymorphisms, allowing the comparison of alleles, are represented by rectangles. (b) Methylation profile of the promoter region of *H19* in various samples determined by bisulfite sequencing. PBL, peripheral blood leukocytes; NT, normal testis tissue; ML, testicular malignant lymphoma tissue; SE, seminomatous TGCT tissue; NSE, non-seminomatous TGCT tissue. The number of each tissue represents the serial code number of our laboratory. The histological components of non-seminomatous TGCTs are shown within parenthesis. Slashes separate the histological compositions of the mixed type TGCTs: the dominant histological component is shown on the left. TGCT histology abbreviations: SE, seminoma; EC, embryonal carcinoma; YST, yolk sac tumor; TE, teratoma; CHO, choriocarcinoma; Rhab, rhabdomyosarcoma.

demonstrated differential methylation at the two regions (126ML and 128ML; Figures 1b and 2b). On the contrary, all TGCT tissues, both seminomas and non-seminomas, showed predominant unmethylation at the

two regions: specifically, two out of two informative seminomatous TGCT samples and three out of the three informative non-seminomatous TGCT samples demonstrated biallelic unmethylation at the promoter region of

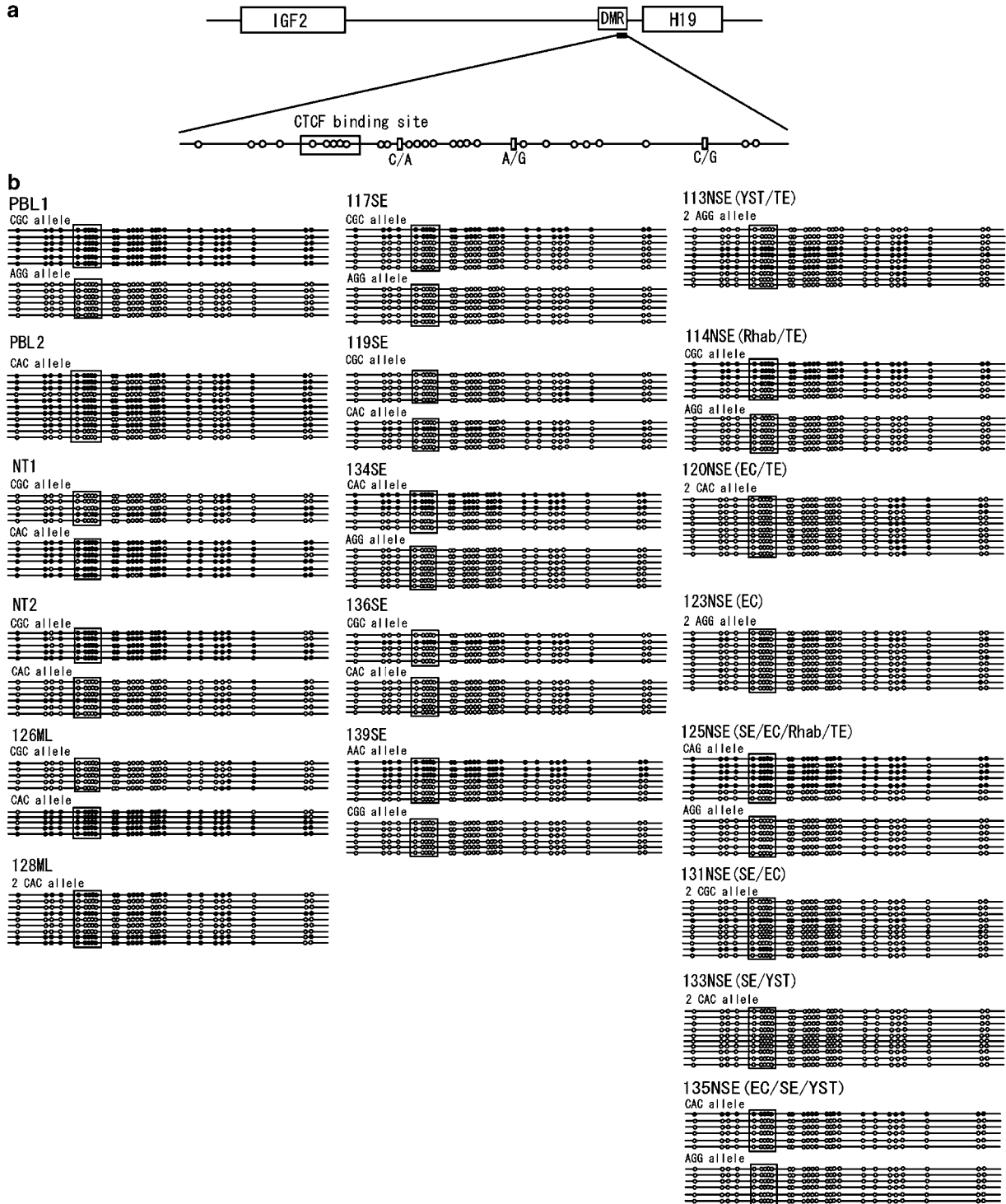


Figure 2 Methylation status of individual CpG sites upstream of *H19*, encompassing the sixth CTCF-binding site. (a) Distribution of CpG dinucleotides upstream of *H19*, encompassing the 6th CTCF-binding site. The 27 CpG sites analysed by bisulfite sequencing are magnified and represented by open circles. The CTCF binding region is boxed. The locations of polymorphisms, allowing the comparison of alleles, are represented by rectangles. (b) Methylation profile upstream of *H19*, encompassing the sixth CTCF-binding site in various samples determined by bisulfite sequencing. The same samples as in Figure 1 were used.

H19 (Figure 1b). Similarly, five out of five informative seminomatous TGCT samples and three out of three informative non-seminomatous TGCT samples demonstrated biallelic unmethylation in the region encompass-

ing the sixth CTCF-binding site (Figure 2b). The other non-polymorphic TGCT samples, both seminomas and non-seminomas, showed predominant unmethylation at the promoter region and the CTCF-binding site

upstream of *H19* (Figures 1b and 2b). This unmethylated profile was stable in the two TGCT samples with malignant transformation (114NSE and 125NSE). The methylation profile of *H19* in each sample is summarized in Table 1.

Methylation patterns of IGF2 is mosaic in TGCTs

Based on the predominant unmethylation profile of *H19* in TGCTs, we analysed *IGF2* DMR located on exons 2 and 3 (Sullivan *et al.*, 1999; Figure 3a). This region contained one polymorphic site and five of the 19 samples were informative for this site. In the PBLs, a similar differential methylation pattern to *H19* was observed. In normal testicular tissues, this region was predominantly methylated. Two malignant lymphoma tissues demonstrated hypomethylation (Figure 3b). In TGCT tissues, methylation erasure at *IGF2* was not clear. The pattern of methylation at this region in TGCTs was mosaic and inconsistent, sample to sample, showing unmethylation (117SE, 119SE, 139SE, 114NSE and 125NSE), hemimethylation (136SE) and mosaic with methylated and unmethylated CpG sites (134SE, 113NSE, 120NSE, 123NSE, 131NSE, 133NSE and 135NSE) (Figure 3b). The methylation profile of *IGF2* in each sample is summarized in Table 1.

Predominant unmethylation at the promoter and the CTCF-binding site upstream of H19 is required, but not sufficient for biallelic expression of H19 in TGCTs

Based on the predominant unmethylation at both the promoter and the six CTCF-binding site upstream of *H19*, we analysed allele-specific expression of *H19* in TGCTs. Before the analysis of *H19* expression, we found conventional primer design encompassing two different exons is not enough to eliminate potential DNA amplification because *H19* genes have short introns. In order to eliminate DNA amplification, we designed a pair of novel reverse transcriptase–polymerase chain reaction (RT–PCR) primer pairs (Figure 4a). RT–PCR data of the TGCT samples are shown in Figure 4b. PBLs, normal testis and malignant lymphoma tissues demonstrated the absence of *H19* expression. Both negative and positive expression patterns were observed in TGCT samples (Figure 4b, Table 1). TGCT samples with positive *H19* transcripts and heterozygosity at the *RsaI* site were analysed for allelic expression. The results showed both mono- and biallelic expression in TGCT samples with positive *H19* expression (Figure 4c, Table 1). Thus, our data showed that null expression, monoallelic expression and biallelic expression were observed in TGCTs, although the promoter and the CTCF-binding site upstream of *H19* remained unmethylated.

Biallelic expression of H19 results in null expression of IGF2 in TGCTs

In consideration of the hypothesis that the sixth CTCF-binding site upstream of *H19* functions as the *IGF2* DMR, we examined how the unmethylated DNA profiles of the CTCF-binding site upstream of *H19*

and expression patterns of *H19* influence patterns of *IGF2* expression. First, we studied the expression of *IGF2* in TGCTs. Similar to the analysis of *H19*, we evaluated *IGF2* expression by single PCR using an exon-connection primer pair to avoid overdiagnosis of *IGF2* expression. PBLs, normal testis and malignant lymphoma tissues demonstrated an absence of *IGF2* expression. Six TGCT tissues were positive for *IGF2* expression, whereas the other seven TGCT tissues were negative (Figure 5b, Table 1). For the five TGCTs with biallelic expression of *H19* (117SE, 139SE, 114NSE, 125NSE, and 135NSE), *IGF2* expression was negative (Figure 5b, Table 1). For the two TGCTs with monoallelic expression of *H19* (134SE and 133NSE) where the *IGF2* *ApaI* site was polymorphic, both showed monoallelic expression of *IGF2* (Figure 5c and Table 1). In these two cases, expression of *IGF2* and *H19* appeared to be re-established even though the methylation patterns at the promoter and the CTCF-binding site upstream of *H19* remain unmethylated.

BORIS expression is heterogeneous in TGCTs although the methylation imprint at H19 is erased

BORIS is a candidate factor for epigenetic reprogramming in the male germ line (Klenova *et al.*, 2002; Loukinov *et al.*, 2002). In order to study whether *BORIS* is involved in epigenetic reprogramming in TGCTs, we studied the expression of *BORIS* in the present series of samples. PBLs and malignant lymphoma tissues showed null expression of *BORIS*, whereas normal testis tissues showed positive expression (Figure 6 and Table 1). *BORIS* expression patterns were heterogeneous in TGCTs: positive and null expression was observed in both seminomatous and non-seminomatous TGCTs (Figure 6 and Table 1). *BORIS* expression was positive in all the TGCTs with biallelic *H19* expression and lack of *IGF2* expression, whereas *BORIS* expression was absent in a TGCT sample with biallelic *IGF2* expression and lack of *H19* expression (Table 1).

On the contrary, expression of *CTCF* was ubiquitously observed in all the TGCT tissues as well as normal testis tissues and PBLs (Figure 6 and Table 1).

Discussion

The present data have shown that methylation imprint at the promoter and CTCF-binding site upstream of *H19* are predominantly erased in both seminomatous and non-seminomatous TGCTs, whereas differential methylation is observed in testicular lymphomas. TGCTs possess a pluripotential nature and display protean histology from germ cells to embryonal and somatic cell differentiation. TGCTs are occasionally known to transform into somatic cancer (e.g., rhabdomyosarcoma). This histological change is a well-described entity called ‘malignant transformation’. Our data demonstrate that the unmethylated status of *H19* is also present in TGCTs with ‘malignant transformation’.

Table 1 Summary of epigenetic profile at *H19* and *IGF2* in TGCTs

Sample category	Sample ^b	Methylation status of <i>H19</i> ^a		Genotyping and allelic expression of <i>H19</i>			Methylation status of <i>IGF2</i> ^a		Genotyping and allelic expression of <i>IGF2</i>		BORIS expression	CTCF expression	
		Methylation at the promoter of <i>H19</i>	Methylation at the sixth CTCF-binding site of <i>H19</i>	Expression of <i>H19</i>	<i>RsaI</i> polymorphism at <i>H19</i>	Allelic expression of <i>H19</i> ^c	Methylation at <i>IGF2</i>	Expression of <i>IGF2</i>	<i>ApaI</i> polymorphism at <i>IGF2</i>	Allelic expression of <i>IGF2</i> ^c			
Peripheral lymphocytes	PBL1	Half Met	Half Met	–	AA	ND	Half Met	–	CC	ND	–	+	
	PBL2	Half Met	Half Met	–	AB	ND	Half Met	–	CC	ND	–	+	
	Normal testis tissues	NT1	Half Met	Half Met ^d	–	BB	ND	Half Met	–	CC	ND	+	+
		NT2	Half Met	Half Met ^d	–	BB	ND	Half Met	–	CC	ND	+	+
		117SE	UnMet	Biallelic UnMet	+	AB	Biallelic	UnMet	–	CD	ND	+	+
119SE	Biallelic UnMet	Biallelic UnMet	+	BB	ND	Biallelic UnMet	–	CD	ND	+	+		
Seminomatous TGCT tissues	134SE	Biallelic UnMet	Biallelic UnMet	+	AB	Monoallelic	Mosaic	+	CD	Monoallelic	–	+	
	136SE	UnMet	Biallelic UnMet	–	AA	ND	Half Met	+	CD	Biallelic	–	+	
	139SE	UnMet	Biallelic UnMet	+	AB	Biallelic	UnMet	–	CD	ND	+	+	
	113NSE (YST/TE)	UnMet	UnMet	–	AA	ND	Mosaic	+	DD	ND	–	+	
	114NSE (Rhab/TE)	Biallelic UnMet	Biallelic UnMet	+	AB	Biallelic	Biallelic UnMet	–	DD	ND	+	+	
	120NSE (EC/TE)	Biallelic UnMet	UnMet	+	BB	ND	Mosaic	–	CC	ND	–	+	
	123NSE (EC)	UnMet	UnMet	–	AA	ND	Mosaic	+	DD	ND	+	+	
Non-seminomatous TGCT tissues	125NSE (SE/EC/Rhab/TE)	Biallelic UnMet	Biallelic UnMet	+	AB	Biallelic	UnMet	–	CC	ND	+	+	
	131NSE (SE/EC)	UnMet	UnMet	–	BB	ND	Mosaic	+	DD	ND	–	+	
	133NSE (SE/YST)	UnMet	UnMet	+	AB	Monoallelic	Mosaic	+	CD	Monoallelic	+	+	
	135NSE (EC/SE/YST)	UnMet	Biallelic UnMet	+	AB	Biallelic	Mosaic	–	DD	ND	+	+	
	126ML	Half Met	Half Met	–	AA	ND	UnMet	–	DD	ND	–	+	
Testicular malignant lymphoma tissues	128ML	Half Met	Half Met	–	AA	ND	UnMet	–	CC	ND	–	+	

^aMethylation status of each region is shown as: Biallelic Unmet, unmethylated clones were observed in both alleles; Unmet, two alleles were not informative for the polymorphisms, but unmethylated clones were predominantly observed; Half Met, one allele was methylated and the other allele was unmethylated or an equal ratio between methylated and unmethylated clones was observed. ^bSamples (peripheral lymphocytes, normal testis tissues, testicular germ cell tumors (TGCTs) tissues and testicular malignant lymphoma tissues) corresponding to Figures 1–3 are shown. SEs, pure seminomatous TGCT tissues; NSEs, non-seminomatous TGCT tissues; MLs, testicular malignant lymphoma tissues. The number of each testicular tumor represents the registration number of our laboratory. The histological components of non-seminomatous TGCTs are shown within parenthesis. Slashes separate the histological compositions of the mixed type TGCTs: the dominant histological component is shown on the left. TGCT histology abbreviations: SE, seminoma; EC, embryonal carcinoma; YST, yolk sac tumor; TE, teratoma; CHO, choriocarcinoma; Rhab, rhabdomyosarcoma. ^cAllelic expression of *H19* and *IGF2* is shown as: Biallelic, biallelic expression; Monoallelic, monoallelic expression; ND, not determined because transcripts were not detected by RT-PCR or DNA was not informative even though transcripts were positive by RT-PCR. ^dHalf Met, Potentially one allele was methylated and the other allele was unmethylated, but a minor proportion of biallelic methylation was observed. Mosaic, each clone was composed of both multiple methylated and unmethylated CpG sites.

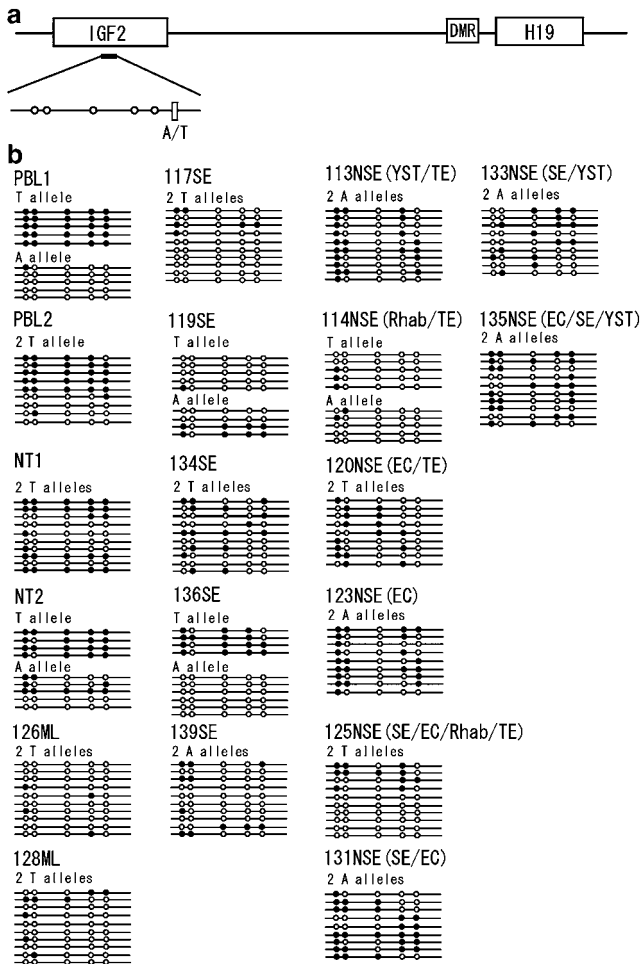


Figure 3 Methylation status of individual CpG sites upstream of *IGF2*, spanning exons 2 and 3. (a) Distribution of CpG dinucleotides upstream of *IGF2*, spanning exons 2 and 3. The five CpG sites analysed by bisulfite sequencing are magnified and represented by open circles. The locations of polymorphisms, allowing the comparison of alleles, are represented by rectangles. (b) Methylation profile upstream of *IGF2*, spanning exons 2 and 3, in various samples as determined by bisulfite sequencing. The same samples as in Figure 1 were used.

Epigenetic alterations in the 11p15.5 imprinted gene cluster are frequent in human cancers and are associated with disordered imprinting of *IGF2* and *H19* (Ogawa et al., 1993; Rainier et al., 1993; Moulton et al., 1994; Steenman et al., 1994; Taniguchi et al., 1995; Feinberg and Tycko, 2004). Loss of imprinting leads to pathological biallelic expression of *IGF2* in Wilms' tumors (Ogawa et al., 1993; Rainier et al., 1993). This abnormality in Wilms' tumors is inevitably linked to a gain in methylation, localized to the 5' sequences and transcribed region of the closely linked and reciprocally imprinted *H19* gene (Moulton et al., 1994; Steenman et al., 1994; Taniguchi et al., 1995).

Recently, the methylation status of the binding site of insulator protein, *CTCF*, in the upstream region of *H19* has been suggested to be critical in the regulation of the *H19/IGF2* locus (Bell and Felsenfeld, 2000; Hark et al., 2000). Allelic expression of *H19* and *IGF2* is regulated

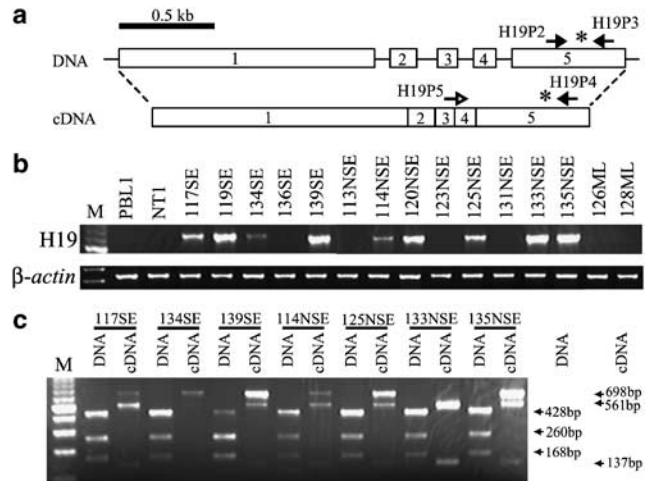


Figure 4 Genotyping, RT-PCR and allelic analysis of *H19* expression. (a) Design of primer pairs encompassing the *RsaI* polymorphic site of *H19* at exon 5 for genotyping and RT-PCR. The asterisk indicates the *RsaI* site. For genotyping, primer pairs H19P2 and H19P3 were used. For allelic analysis of *H19* expression, primer pairs H19P5 and H19P4 were used (Note that the forward primer P5 encompasses exons 3 and 4 in order to abolish DNA amplification.) (b) Expression of *H19* in various samples. The same samples as in Figure 1 were used. Top: RT-PCR analysis of *H19* expression; bottom: RT-PCR using β -actin primers as a control. (c) Allelic analysis of *H19* expression in various samples. Samples with positive *H19* transcripts, as shown in Figure 4b, and heterozygous at the *H19 RsaI* restriction site were analysed for allelic expression. Genomic PCR products with primer pairs H19P2 and H19P3 and *RsaI* restriction-digested fragments are shown in the left of each sample (lane DNA). Note that both the undigested band (428 bp) and digested bands (168 and 260 bp) are seen. Products of RT-PCR with primer pairs H19P4 and H19P5 and *RsaI* restriction-digested fragments are shown in the right of each sample (lane cDNA). Note 117SE, 139SE, 114NSE, 125NSE and 135NSE demonstrate both an undigested band (698 bp) and digested bands (561 and 137 bp), indicating biallelic expression of *H19*; 134SE demonstrates only an undigested band and 133NSE demonstrates only digested bands, indicating mono-allelic expression of *H19*.

by the binding of *CTCF* insulators to parent-specific DNA methylation sites in an imprinting control center (ICR) located between the two genes in mouse (Bell and Felsenfeld, 2000; Hark et al., 2000). The 5' region of human *H19* contains seven *CTCF*-binding sites (Hark et al., 2000), but only the sixth of the seven *CTCF*-binding sites has been demonstrated to have allele-specific methylation in humans (Takai et al., 2001). Hypermethylation of the sixth *CTCF*-binding site has been reported in Wilms' tumor with biallelic expression of *IGF2* (Cui et al., 2001). So far, the methylation profiles of *H19* have been reported not only in Wilms' tumors but also in osteosarcoma, colorectal cancer and bladder cancer. Similar to Wilms' tumors, hypermethylation of *H19* results in biallelic expression of *IGF2* in colorectal cancer (Nakagawa et al., 2001). Hypomethylation of the sixth *CTCF* has been reported in some of the osteosarcomas (Ulaner et al., 2003) and bladder cancer (Takai et al., 2001). However, the promoter region of *H19* is hemimethylated in osteosarcomas with hypomethylation of *CTCF*-binding sites (Ulaner et al.,

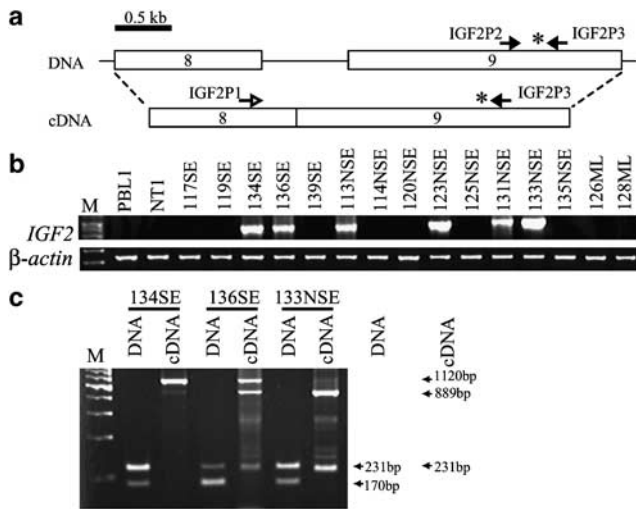


Figure 5 Genotyping, RT-PCR and allelic analysis of *IGF2* expression. (a) Design of primer pairs encompassing the *ApaI* polymorphic site of *IGF2*, exon 9, for genotyping and RT-PCR. The asterisk indicates the *ApaI* site of *IGF2* in exon 9. For genotyping, primer pairs IGF2P2 and IGF2P3 were used. For allelic analysis of *IGF2* expression, primer pairs IGF2P1 and IGF2P3 were used. (b) Expression of *IGF2* in various samples. The same samples as in Figure 1 were used. Top: RT-PCR analysis of *IGF2* expression; bottom: RT-PCR using β -actin primers as a control. (c) Allelic analysis of *IGF2* expression in various samples. Samples with positive *IGF2* transcripts, as shown in Figure 5b, and heterozygous at the *IGF2* *ApaI* restriction site were analysed for allelic expression. Genomic PCR products with primer pairs IGF2P2 and IGF2P3 and *ApaI* restriction-digested fragments are shown in the left of each sample (lane DNA). Note that both digested (170 bp) and undigested bands (231 bp) are seen. Products of RT-PCR with primer pairs IGF2P1 and IGF2P3 and *ApaI* restriction-digested fragments are shown in the right of each sample (lane cDNA). Note 136SE demonstrates both an undigested band (1120 bp) and digested bands (889 and 231 bp), indicating biallelic expression of *IGF2*; 134SE demonstrates only undigested bands and 133NSE demonstrates only digested bands, both indicating monoallelic expression of *IGF2*.

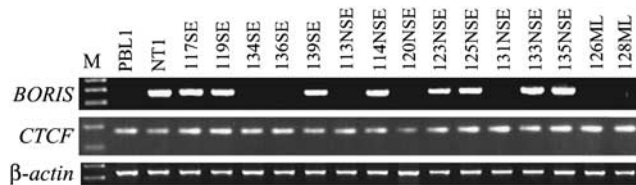


Figure 6 Expression of *BORIS* and *CTCF*. Expression of *BORIS* and *CTCF* in various samples. The same samples as in Figure 1 were used. RT-PCR analysis of *BORIS* expression (top) and *CTCF* expression (middle). Bottom: RT-PCR using β -actin primers as a control.

2003). In bladder cancer with hypomethylated CTCF-binding site, the neighboring CpG sites are significantly methylated (Takai *et al.*, 2001). These data suggest that hypomethylation of the sixth CTCF-binding site of *H19* in somatic neoplasms appear to be owing to a ‘gain of hypomethylation’ from which normal somatic tissues carry hemimethylation.

The patterns of methylation at the promoter and CTCF-binding site upstream of *H19* observed in

TGCTs are distinct from those reported in other types of neoplasms because CpG sites at the promoter and CTCF-binding site upstream of *H19* are thoroughly unmethylated in TGCTs. Thus, we propose the patterns of methylation of *H19* in TGCTs as ‘erasure of methylation’ by contrast with ‘gain of hypomethylation’ in somatic neoplasms. The region between exons 2 and 3 of *IGF2* has been suggested as a putative DMR (Sullivan *et al.*, 1999). We confirmed this region is hemimethylated in normal PBLs. Different from the upstream region of *H19*, methylation erasure at this region was variable in TGCTs: some seminoma samples showed unmethylation, whereas most of the TGCTs were mosaic for methylated and unmethylated CpG sites at *IGF2*.

The present data also show that allelic expression patterns of *H19* and *IGF2* in TGCTs are different from other type of neoplasms (Moulton *et al.*, 1994; Steenman *et al.*, 1994; Taniguchi *et al.*, 1995; Cui *et al.*, 2001; Nakagawa *et al.*, 2001; Ulaner *et al.*, 2003): null expression, monoallelic expression and biallelic expression of both *H19* and *IGF2* were observed in TGCTs with consistent unmethylated DNA profiles of *H19* (Table 1). Biallelic expression of both *IGF2* and *H19* has been reported in TGCTs of adolescents (van Gurp *et al.*, 1994; Nonomura *et al.*, 1997; Verkerk *et al.*, 1997) and pediatrics (Ross *et al.*, 1999). We also observed biallelic expression of *IGF2* and *H19* in the present series; however, our data did not show the conflicting expression patterns of *H19* and *IGF2* reported in the previous study (van Gurp *et al.*, 1994; Nonomura *et al.*, 1997). The common expression patterns in TGCTs were biallelic expression of *H19* and null expression of *IGF2* in the present study (Table 1). The patterns of *H19/IGF2* expression were in contrast to those in Wilms’ tumors (Ogawa *et al.*, 1993; Rainier *et al.*, 1993; Moulton *et al.*, 1994; Steenman *et al.*, 1994; Taniguchi *et al.*, 1995; Feinberg and Tycko, 2004).

Our results imply that predominant unmethylation at the promoter and the CTCF-binding site upstream of *H19* is required, but not sufficient for biallelic expression of *H19* in TGCTs. The data suggest that factors other than methylation contribute to transcriptional regulation of the imprinted genes in TGCTs. We have already reported similar discordance between expression and methylation in TGCTs at *XIST* (Kawakami *et al.*, 2004a) and cancer testis antigens (Zhang *et al.*, 2005).

Jaenisch (1997) has suggested that DNA methylation has no role in PGC or germline lineages. The present data combined with our previous data (Kawakami *et al.*, 2003, 2004a; Zhang *et al.*, 2005) support this hypothesis in TGCTs.

Loss of allele-specific methylation imprints has also been observed in both male and female PGCs of the mouse (Szabo and Mann, 1995a; Tada *et al.*, 1998). In particular, *H19* is unmethylated both in the paternal and maternal allele in mouse PGCs, whereas gain of methylation occurs prospermatogonia onward (Davis *et al.*, 2000). These data support the theory that pre-existing imprints are erased in the germ line by this stage. By analysing microdissected individual cells at

different stage of human male germ cell development, Kerjean *et al.* (2000) have shown that fetal spermatogonia carry predominant unmethylation at the DMRs of *H19*, although adult testis germ cells (spermatogonia onward) demonstrate significant methylation at this region. In this study, normal testis showed potentially half methylation, but included a minor population with biallelic methylation at the CTCF-binding site upstream of *H19*. Based on the data by Davis *et al.* (2000), the population with biallelic methylation at *H19* may represent spermatocytes or spermatozoa in normal testicular parenchyma. In the light of previous human and mouse data (Davis *et al.*, 2000; Kerjean *et al.*, 2000), our results provide direct evidence that both seminomatous and non-seminomatous TGCTs share similar epigenetic profiles to those observed in fetal germ cells, probably PGCs, but not adult germ cells. This might imply TGCTs originate from fetal germ cells.

A previous report suggested that *BORIS* acts to remove methylation marks in the male germ line because the onset of *BORIS* expression correlates with the timing of genome-wide demethylation during male germline development, and *BORIS* is a paralog of *CTCF* (Loukinov *et al.*, 2002). Aberrant expression of *BORIS* has been suggested in different tumors (Klenova *et al.*, 2002). In osteosarcoma tissues, *BORIS* expression is observed predominantly among tumors with biallelic hypomethylation of the CTCF-binding site upstream of *H19* (Ulaner *et al.*, 2003). Our data show that in both seminomatous and non-seminomatous TGCTs, the patterns of *BORIS* expression are heterogeneous, whereas the methylation imprint at the promoter and CTCF-binding site upstream of *H19* are constantly erased.

These results imply that *BORIS* expression may not function in the reprogramming of methylation, at least in TGCTs. However, there is a possibility that *BORIS* is required for the initiation of methylation erasure of imprinted genes, but is not necessary for maintenance of the unmethylated state of DNA. In the present data, *BORIS* expression was positive in all the TGCTs with biallelic *H19* expression and lack of *IGF2* expression, whereas *BORIS* expression was absent in a TGCT sample with biallelic *IGF2* expression and lack of *H19* expression (Table 1). The data might indicate that *BORIS* possesses insulator function without methylation in germ line, although possible reciprocal expression patterns of *BORIS/CTCF* should be tested by further analysis using microdissection.

In conclusion, the present data show that TGCTs carry distinctive epigenetic profiles at the core-imprinting domain of *H19/IGF2* from other neoplasms of somatic cell origin. The data imply that both seminomatous and non-seminomatous TGCTs show methylation erasure at the imprinting domain same as that in fetal germ cells. It remains to be elucidated whether the unique epigenetic profile of TGCTs reflects only that in the precursor cells of TGCTs or whether it also contributes to TGCT development.

Materials and methods

Tumor samples and pathological data

Thirteen primary TGCT specimens (five seminomas and eight non-seminomatous TGCT tissues) and two primary non-Hodgkin's lymphoma of the testis (diffuse large-type non-Hodgkin's lymphomas) were surgically resected at Shiga University of Medical Science (Shiga, Japan). Eight non-seminomatous TGCT samples with different histology, including two TGCT samples with malignant transformation, were selected. Specimens approximately 10 mm in diameter were bisected, with one-half being frozen immediately and stored at -80°C until subsequent analysis. The remaining half was fixed with buffered formalin for histopathological diagnosis, allowing the selection of samples with a neoplastic cellularity exceeding 70%. Tumors were classified according to the World Health Organization's classification for testicular cancer. After histological confirmation, frozen tissues were separated into two for DNA and RNA extraction. Two normal testis tissues of young adults were obtained through orchiectomy owing to testicular injury. Normal spermatogenesis of the testis tissues was confirmed by histological examination. PBLs from two healthy volunteers were also included in this study. Written informed consent was obtained in advance for all human tissue samples. Sample collection was monitored and approved by the institutional review board.

DNA/RNA extraction and cDNA synthesis

DNA was extracted from PBLs, and tissues samples using QIAamp DNA Extraction Kits (Qiagen, Valencia, CA, USA). Total RNA was extracted from PBLs and tissue samples using TRIzol reagent RNA extraction kit (Invitrogen, CA, USA). All RNA preparations were treated with DNase I for 15 min at room temperature immediately before conversion to cDNA using reagents from Life Technologies Superscript II kit (Rockville, MD, USA).

Treatment of DNA with sodium bisulfite

Bisulfite treatment was performed according to the method of Clark *et al.* (1994) with alterations detailed by Frevel *et al.* (1999). Before bisulfite treatment, 2 μg of genomic DNA were digested for 4 h at 37°C with *HindIII*. Digested DNA was ethanol precipitated and resuspended in 40 μl of H_2O . The bisulfite reaction, under mineral oil, was performed at 60°C for 16 h in 525 μl total volume containing 2.4 M sodium bisulfite (Sigma) and 123 mM hydroquinone (Sigma). Reactions were desalted using a QIAEX II gel extraction kit (Qiagen, Valencia, CA, USA). DNA was eluted in 50 μl of H_2O , incubated with 5 μl of 3 M NaOH for 15 min at 37°C , neutralized with ammonium acetate (final concentration of 3 M) and ethanol precipitated. Bisulfite-treated DNA was then resuspended in 25 μl of H_2O and stored at -20°C .

Cloning and sequencing of bisulfite-treated DNA

Bisulfite genomic sequencing was used to analyse the methylation patterns of the promoter region of *H19* DMR and the CTCF-binding sites of *H19* and *IGF2* DMR.

The bisulfite-treated DNA was amplified by PCR, cloned and sequenced using TOPO TA Cloning Kit (Invitrogen). PCRs were performed in 25 μl volumes using GeneAmp reaction buffer II (Applied Biosystems, Foster City, CA, USA) under the following conditions: 1.5 mM MgCl_2 , 200 μM each deoxynucleotide triphosphate, 0.8 μM final concentration of each primer and 1 U of AmpliTaq Gold polymerase (Applied Biosystems). To obtain the PCR products for the promoter region of *H19* DMR and *IGF2* DMR, nested or

heminested PCRs were performed using 5 μ l of bisulfite-treated DNA in the first amplification (25 μ l total volume) and 5 μ l of this PCR product as the template in the second amplification (50 μ l total volume). PCRs were performed on a Peltier Thermal Cycler-200 (MJ Research, Watertown, MA, USA) using PCR cycling programs with annealing temperatures of 50°C for the first round of PCR and 55°C for the second round of PCR. For the CTCF-binding sites of *H19*, single PCR was performed at annealing temperatures of 55°C. Successful PCR products were then cloned and sequenced as described above. Ten to 12 random clones were isolated from a PCR amplicon and sequenced.

Primer pairs for the promoter region of *H19* were: outer primer pairs – H19-F1, 5'-CTC(A/G)CCAATCTCCACTC CACTCCCAACC (9346–9373, AF125183); H19-R1, 5'-TGTATATATTTTGTATATGGTTGG (original, 9747–9770, AF125183); and inner primer pairs – H19-F2, 5'-AACCTAA AAAAATCTATAAAAC (original, 9389–9410, AF125183); H19-R2, TTTTGGGGATT(C/T)GGATGGTATAGAGGGT (9704–9731, AF125183). Primer pairs upstream of *H19*, encompassing the sixth CTCF-binding site, were: CTCF6-F, 5'-GTAGGGTTTTTGGTAGGTATAGAGT (7834–7858, AF125183); CTCF6-R, 5'-CACTAAAAACAATTATCA ATTC (8314–8338, AF125183). Primer pairs for *IGF2* DMR were: outer primer pairs – BIS IGF2-F1, 5'-GGTGGTTAG TAGGTATAGGGAGGTA (64972–64996, AC006408); BIS IGF2-R1, 5'-CTCCTTTAAAACACTACACAAAACCACT (65287–65310, AC006408); and inner primer pairs – BIS IG F2-F3, 5'-TTTATTTGTAAAATGGTGTATATATGT (65011–65037, AC006408); BIS IGF2-R3, 5'-TAAAACCTTTACAA AAAAAATAAAT (65261–65286, AC006408). Accession number and corresponding nucleotide number of each primer is shown within parenthesis.

Analysis of *H19* *RsaI* polymorphism

H19 *RsaI* heterozygosity was determined in DNA of TGCTs, testicular non-Hodgkin's lymphomas, normal testis tissues and PBLs using primer pairs P2 and P3 (Figure 4a). One microliter of the PCR products was mixed with 2 U of *RsaI* (Invitrogen, CA, USA) in a total volume of 20 μ l, and digested at 37°C for 6 h. Products were electrophoresed on 2% agarose gel and visualized using a Phosphorimager. The results of *H19* genotyping are shown in Table 1. Sequences of the primer pair were: H19P2, 5'-ACCCCTGCGGTGGACGGTT (12254–12273, AF125183); H19P3, 5'-TGGAATGCTTGAAGCT GCT (12662–12681, AF125183). Accession number and corresponding nucleotide number of each primer are shown within parenthesis.

RT-PCR and allelic analysis of *H19* expression

For subsequent RT-PCR and allelic analysis of *H19* expression, we designed a new method to avoid overdiagnosis of biallelic expression. In order to obtain accurate RT-PCR results exclusively derived from cDNA, it is essential to eliminate DNA products. A previous report indicated that exon-connection PCR should be used routinely to analyse allele specificity of imprinted genes (Yun *et al.*, 1999). If exon-connection RT-PCR is not used, genomic DNA may be co-amplified during the PCR and this artifact cannot be completely excluded, despite using RT minus samples as negative controls. The possibility of amplifying genomic DNA is increased particularly if nested-PCR is employed. We used single exon-connection PCR to evaluate the expression of *H19*; however, conventional primer design encompassing two different exons may not eliminate DNA amplification because *H19* genes have short introns (GenBank Accession number:

AF125183). Indeed, we initially tested primer pairs encompassing exons 4 and 5, and the results showed significant DNA amplification (data not shown). Therefore, we designed a new forward primer encompassing exons 3 and 4 to abolish DNA amplification. Locations of primers and the *RsaI* restriction site are shown in Figure 4a. By using these primer pairs, we were able to exclude DNA amplification from DNA samples, thus obtaining convincing results for *H19* expression. PCR reactions were performed by mixing 1 μ l of first-strand cDNAs, 0.8 μ M primers (P4 and P5) and 1 U AmpliTaq DNA polymerase (Amersham) in a total of 25 μ l. A step-down PCR protocol was used: heat activation of 13 min at 95°C followed by three cycles of 30 s at 95°C, 15 s at 74°C and 30 s at 72°C; three cycles of 30 s at 95°C, 15 s at 70°C and 30 s at 72°C; three cycles of 30 s at 95°C, 15 s at 66°C and 30 s at 72°C; three cycles of 30 s at 95°C, 15 s at 62°C and 30 s at 72°C; three cycles of 30 s at 95°C, 15 s at 58°C and 30 s at 72°C; 30 cycles of 30 s at 95°C, 15 s at 55°C and 30 s at 72°C for 30 s, followed by final elongation step of 5 min at 72°C. Samples with positive *H19* transcripts and heterozygous for the *H19* *RsaI* polymorphism were then analysed for allelic expression. Ten microliter of RT-PCR products was mixed with 2 U of *RsaI* (Invitrogen, CA, USA) in a total volume of 20 μ l, and digested at 37°C for 6 h. Products were electrophoresed on 2% agarose gel and visualized using a Phosphorimager. Sequences of the primer pair were: H19P4, 5'-TCGGAGCTTCCAGACTAG (12632–12649, AF125183); H19P5, 5'-AACATGAAA GAAA TGGTGCTA (11854–11863 and 11945–11955, AF125183). Accession number and corresponding nucleotide number of each primer are shown within parenthesis.

Analysis of *IGF2* *ApaI* polymorphism

IGF2 *ApaI* heterozygosity (Figure 5a) was determined in TGCTs, testicular non-Hodgkin's lymphomas, normal testis tissues and PBLs using primer pairs IGF2P2 and IGF2P3 (Figure 5a). Ten microliter of PCR products was mixed with 2 U of *ApaI* (Invitrogen, CA, USA) in a total volume of 20 μ l, and digested at 30°C for 6 h. Products were electrophoresed on 2% agarose gel and visualized using a Phosphorimager. The results of *IGF2* genotyping are shown in Table 1. Sequences of the primer pair were (Ogawa *et al.*, 1993): IGF2P2, 5'-CTTGGACTTTGAGTCAAATTGG (8703–8724, X03562); IGF2P3, 5'-GGTCGTGCCAATTACATTTCA (940646–940666, NT009237). Accession number and corresponding nucleotide number of each primer are shown within parenthesis.

RT-PCR and allelic analysis of *IGF2* expression

Similar to *H19*, we employed single PCR with exon-connection primer pairs to evaluate *IGF2* expression (Figure 5a). The cDNA samples were subject to PCR with primer P1 and P3 (Show Sequence). PCR reactions were performed by mixing 1 μ l of first-strand cDNAs, 0.8 μ M primers (P1 and P3) and 1 U AmpliTaq DNA polymerase (Amersham) in a total of 25 μ l.

The following PCR protocol was used: heat activation of 13 min at 95°C followed by 35 cycles of 30 s at 95°C, 30 s at 55°C and 1 min at 72°C, followed by final elongation step of 5 min at 72°C. Samples with positive *IGF2* transcript and heterozygous at the *IGF2* *ApaI* polymorphism were then analysed for allelic expression. Sequences of the primer pair were (Ogawa *et al.*, 1993): IGF2P1, 5'-TCCTGGAGACG TACTGTGCTA (7583–7603, X03562); IGF2P3, 5'-GGTC GTGCCAATTACATTTCA. Accession number and corresponding nucleotide number of each primer is shown within parenthesis.

RT-PCR of *BORIS* and *CTCF*

Expression of *BORIS* and *CTCF* was assessed by RT-PCR. Pairs of oligonucleotide primers were used to amplify fragments encompassing an intron area in the corresponding genomic sequence in order to differentiate the amplification results from genomic DNA. The sequences were as follows (Loukinov *et al.*, 2002): *BORIS*-F, 5'-CAGGCCCTA CAAGTGTAACGACTGCAA (1019–1045, AF336042); *BORIS*-R, 5'-GCATTCGTAAGGCTTCTCACCTGAGTG (1263–1289, AF336042); and *CTCF*-F, 5'-GAACCCATT

CAGGGGAAAAGC (1487–1507, U25435); *CTCF*-R, 5'-TCGCAAGTGGACACCCAAATC (1487–1507, U25435).

Acknowledgements

This work was supported by Grants-in-aid 16390462 and 17390438 from the Ministry of Education, Culture, Sports, Science and Technology, Japan and Research Grant from Takeda Science Foundation and Research Grant for the Princess Takamatsu Cancer Research Fund (04-23603).

References

- Allen RC, Zoghbi HY, Moseley AB, Rosenblatt HM, Belmont JW. (1992). *Am J Hum Genet* **51**: 1229–1239.
- Barlow DP. (1993). *Science* **260**: 309–310.
- Bartolomei MS, Webber AL, Brunkow ME, Tilghman SM. (1993). *Genes Dev* **7**: 1663–1673.
- Bell AC, Felsenfeld G. (2000). *Nature* **405**: 482–485.
- Brandeis M, Kafri T, Ariel M, Chaillet JR, McCarrey J, Razin A *et al.* (1993). *EMBO J* **12**: 3669–3677.
- Clark SJ, Harrison J, Paul CL, Frommer M. (1994). *Nucleic Acids Res* **22**: 2990–2997.
- Cui H, Niemitz EL, Ravenel JD, Onyango P, Brandenburg SA, Lobanenkova VV *et al.* (2001). *Cancer Res* **61**: 4947–4950.
- Davis TL, Yang GJ, McCarrey JR, Bartolomei MS. (2000). *Hum Mol Genet* **9**: 2885–2894.
- Feinberg AP, Tycko B. (2004). *Nat Rev Cancer* **4**: 143–153.
- Ferguson-Smith AC, Sasaki H, Cattanach BM, Surani MA. (1993). *Nature* **362**: 751–755.
- Frevel MA, Sowerby SJ, Petersen GB, Reeve AE. (1999). *J Biol Chem* **274**: 29331–29340.
- Grant M, Zuccotti M, Monk M. (1992). *Nat Genet* **2**: 161–166.
- Hajkova P, Erhardt S, Lane N, Haaf T, El-Maarri O, Reik W *et al.* (2002). *Mech Dev* **117**: 15–23.
- Hark AT, Schoenherr CJ, Katz DJ, Ingram RS, Levorse JM, Tilghman SM. (2000). *Nature* **405**: 486–489.
- Holstein AF. (1993). *Eur Urol* **23**(Suppl 2): 9–18.
- Huber R, Hansen RS, Strazzullo M, Pengue G, Mazzarella R, D'Urso M *et al.* (1999). *Proc Natl Acad Sci USA* **96**: 616–621.
- Jaenisch R. (1997). *Trends Genet* **13**: 323–329.
- Jinno Y, Sengoku K, Nakao M, Tamate K, Miyamoto T, Matsuzaka T *et al.* (1996). *Hum Mol Genet* **5**: 1155–1161.
- Jorgensen N, Rajpert-DeMeyts E, Graem N, Muller J, Giwercman A, Skakkebaek NE. (1995). *Lab Invest* **72**: 223–231.
- Kafri T, Ariel M, Brandeis M, Shemer R, Urven L, McCarrey J *et al.* (1992). *Genes Dev* **6**: 705–714.
- Kato Y, Rideout III WM, Hilton K, Barton SC, Tsunoda Y, Surani MA. (1999). *Development* **126**: 1823–1832.
- Kawakami T, Okamoto K, Ogawa O, Okada Y. (2004a). *Lancet* **363**: 40–42.
- Kawakami T, Okamoto K, Sugihara H, Hattori T, Reeve AE, Ogawa O *et al.* (2003). *J Urol* **169**: 1546–1552.
- Kawakami T, Zhang C, Taniguchi T, Kim CJ, Okada Y, Sugihara H *et al.* (2004b). *Oncogene* **23**: 6163–6169.
- Kerjean A, Dupont JM, Vasseur C, Le Tessier D, Cuisset L, Paldi A *et al.* (2000). *Hum Mol Genet* **9**: 2183–2187.
- Kirchgesner CU, Warren ST, Willard HF. (1995). *J Med Genet* **32**: 925–929.
- Klenova EM, Morse III HC, Ohlsson R, Lobanenkova VV. (2002). *Semin Cancer Biol* **12**: 399–414.
- Lee J, Inoue K, Ono R, Ogonuki N, Kohda T, Kaneko-Ishino T *et al.* (2002). *Development* **129**: 1807–1817.
- Li E. (2002). *Nat Rev Genet* **3**: 662–673.
- Looijenga LH, Stoop H, de Leeuw HP, de Gouveia Brazao CA, Gillis AJ, van Roozendaal KE *et al.* (2003). *Cancer Res* **63**: 2244–2250.
- Loukinov DI, Pugacheva E, Vatolin S, Pack SD, Moon H, Chernukhin I *et al.* (2002). *Proc Natl Acad Sci USA* **99**: 6806–6811.
- Moller H. (1989). *J Natl Cancer Inst* **81**: 1668–1669.
- Moulton T, Crenshaw T, Hao Y, Moosikasuwan J, Lin N, Dembitzer F *et al.* (1994). *Nat Genet* **7**: 440–447.
- Nakagawa H, Chadwick RB, Peltomaki P, Plass C, Nakamura Y, de La Chapelle A. (2001). *Proc Natl Acad Sci USA* **98**: 591–596.
- Nonomura N, Miki T, Nishimura K, Kanno N, Kojima Y, Okuyama A. (1997). *J Urol* **157**: 1977–1979.
- Ogawa O, Eccles MR, Szeto J, McNoe LA, Yun K, Maw MA *et al.* (1993). *Nature* **362**: 749–751.
- Okano M, Bell DW, Haber DA, Li E. (1999). *Cell* **99**: 247–257.
- Oosterhuis JW, Looijenga LH. (2005). *Nat Rev Cancer* **5**: 210–222.
- Rainier S, Johnson LA, Dobry CJ, Ping AJ, Grundy PE, Feinberg AP. (1993). *Nature* **362**: 747–749.
- Rajpert-De Meyts E, Hanstein R, Jorgensen N, Graem N, Vogt PH, Skakkebaek NE. (2004). *Hum Reprod* **19**: 1338–1344.
- Reik W, Dean W, Walter J. (2001). *Science* **293**: 1089–1093.
- Ross JA, Schmidt PT, Perentesis JP, Davies SM. (1999). *Cancer* **85**: 1389–1394.
- Shiota K, Yanagimachi R. (2002). *Differentiation* **69**: 162–166.
- Skakkebaek NE. (1972). *Lancet* **2**: 516–517.
- Skakkebaek NE, Berthelsen JG, Giwercman A, Muller J. (1987). *Int J Androl* **10**: 19–28.
- Smiraglia DJ, Szymanska J, Kraggerud SM, Lothe RA, Peltomaki P, Plass C. (2002). *Oncogene* **21**: 3909–3916.
- Steenman MJ, Rainier S, Dobry CJ, Grundy P, Horon IL, Feinberg AP. (1994). *Nat Genet* **7**: 433–439.
- Sullivan MJ, Taniguchi T, Jhee A, Kerr N, Reeve AE. (1999). *Oncogene* **18**: 7527–7534.
- Szabo PE, Mann JR. (1995a). *Genes Dev* **9**: 3097–3108.
- Szabo PE, Mann JR. (1995b). *Genes Dev* **9**: 1857–1868.
- Tada T, Tada M, Hilton K, Barton SC, Sado T, Takagi N *et al.* (1998). *Dev Genes Evol* **207**: 551–561.
- Takai D, Gonzales FA, Tsai YC, Thayer MJ, Jones PA. (2001). *Hum Mol Genet* **10**: 2619–2626.
- Taniguchi T, Sullivan MJ, Ogawa O, Reeve AE. (1995). *Proc Natl Acad Sci USA* **92**: 2159–2163.
- Thorvaldsen JL, Duran KL, Bartolomei MS. (1998). *Genes Dev* **12**: 3693–3702.
- Ulaner GA, Yang Y, Hu JF, Li T, Vu TH, Hoffman AR. (2003). *Endocrinology* **144**: 4420–4426.
- Ulbright TM. (1993). *Am J Surg Pathol* **17**: 1075–1091.
- van Gurp RJ, Oosterhuis JW, Kalscheuer V, Mariman EC, Looijenga LH. (1994). *J Natl Cancer Inst* **86**: 1070–1075.

- Verkerk AJ, Ariel I, Dekker MC, Schneider T, van Gurp RJ, de Groot N *et al.* (1997). *Oncogene* **14**: 95–107.
- Villar AJ, Eddy EM, Pedersen RA. (1995). *Dev Biol* **172**: 264–271.
- Vu TH, Li T, Nguyen D, Nguyen BT, Yao XM, Hu JF *et al.* (2000). *Genomics* **64**: 132–143.
- Yun K, Soejima H, Merrie AE, McCall JL, Reeve AE. (1999). *J Pathol* **187**: 518–522.
- Zhang C, Kawakami T, Okada Y, Okamoto K. (2005). *Genes Chromosomes Cancer* **43**: 104–112.
- Zhang Y, Shields T, Crenshaw T, Hao Y, Moulton T, Tycko B. (1993). *Am J Hum Genet* **53**: 113–124.